

Preparation of nanocomposites of polyaniline and inorganic semiconductors

Dmitri Yu. Godovsky,^a Andrei E. Varfolomeev,^a David F. Zaretsky,^a R. L. Nayana Chandrakanthi,^b Andreas Kündig,^c Christoph Weder^c and Walter Caseri*^c

^aRRC "Kurchatov Institute", 123182 Moscow, Russia

^bDepartment of Physics, University of Peradeniya, Peradeniya, Sri Lanka

^cDepartment of Materials, Institute of Polymers, ETH Zürich, CH-8092 Zürich, Switzerland

Received 4th April 2001, Accepted 16th July 2001

First published as an Advance Article on the web 6th September 2001

Nanocomposites of polyaniline (PANI) and the semiconducting metal sulfides CdS and Cu₂S were prepared from the respective metal trifluoromethanesulfonates co-dissolved in *N*-methylpyrrolidone. Metal sulfide particles with typical diameters of 1–2 nm formed *in situ* upon addition of Li₂S; the nanocomposites were subsequently isolated by co-precipitation. UV/VIS absorption spectra suggest that the PANI–CdS nanocomposites are stable in the air, while PANI was found to degrade in the presence of Cu₂S. Appreciable photovoltaic effects were measured on multilayer devices based on Al/nanocomposite/Cd_{1-x}Zn_xO and Al/nanocomposite/C₆₀/Cd_{1-x}Zn_xO. In the absence of the C₆₀ layer, both open circuit photovoltage (U_{oc}) and short circuit photocurrent (I_{sc}) were found to increase substantially with increasing CdS content, while in the presence of a C₆₀ layer, more complex behavior was observed.

Introduction

Polyaniline (PANI) is one of the most frequently investigated (semi)conducting polymers for use in electronic applications.^{1,2} Its properties can be tailored, *e.g.*, by changing the oxidation state, the addition of appropriate additives, such as acids, or through blending with other organic or inorganic semiconductors. Here, we focus on the incorporation of inorganic nanosize semiconducting particles, which recently has been used as a tool to create materials with novel electronic properties.^{3–8} In contrast to reported materials that are comprised of large particles, polymeric systems containing colloids with dimensions below 50 nm exhibit reduced light scattering effects and, thus, are attractive for optical applications. In addition, the large internal interface area in nanocomposites enables an efficient separation of photo-induced charges, which is important for photovoltaic applications, and the number of carrier traps caused by the so-called grain boundaries between the particles and the matrix is reduced.^{9,10} It is therefore expected that useful photoconducting nanocomposites can be created by combination of PANI as a p-type semiconductor and n-type semiconductor nanoparticles, such as CdS or PbS. In fact, it already has been shown that nanocomposites of PANI and PbS can operate as photovoltaic cells in which the charges generated under illumination in the PbS colloids are subsequently transported by the polymer.¹¹ Composites of PANI and TiO₂ with an average particle size around 21 nm also exhibit photoconductivity.¹² Upon irradiation, electrons are thought to be transferred from PANI to TiO₂. Subsequently, the charges move to the respective electrodes.¹²

Unfortunately, options for the processing of PANI are limited, since this polymer decomposes prior to melting and is only soluble in a few solvents, such as strong acids and *N*-methylpyrrolidone (NMP). This situation severely restricts the synthetic routes for the preparation of PANI nanocomposites. Most nanocomposites based on a PANI matrix have been fabricated *via in situ* polymerization in an aqueous solution containing the colloidal particles or their precursors.^{11,13–17} The inorganic colloids required for the preparation of nanocomposites are typically prepared *in situ*, since inorganic

nanoparticles strongly agglomerate upon isolation. Metal sulfide nanoparticles, which are of interest within the scope of this report, are generally produced by reaction of the respective metal ions with hydrogen sulfide or sodium sulfide in aqueous solution,^{18–25} because common metal compounds suitable for *in situ* synthesis of the particles are usually insoluble in organic solvents. The modification of the surface of inorganic particles with organic compounds dramatically diminishes the specific surface energy. As a consequence, such colloids can be isolated and the primary particles can be redispersed in a broad range of solvents and, thus, can be incorporated in a variety of polymers. Accordingly, nanocomposites of surface-modified γ -Fe₂O₃ and polyaniline were prepared by mixing these components in NMP;²⁶ this technique has also been used for the preparation of nanocomposites with CdS and polymers other than PANI.^{9,13,27–30} However, an organic surface layer may stifle charge transport from the particle core to the polymer matrix or to neighboring particles and, in addition, may change the particles' electronic characteristics.²⁷ Thus, we set out to develop a new method for the preparation of nanocomposites of PANI and semiconducting metal sulfides. We have chosen CdS as an n-type and Cu₂S as a p-type semiconductor. The new route is based on metal trifluoromethanesulfonates as NMP-soluble precursors for the *in situ* preparation of metal sulfides. Since ionic byproducts stemming from the synthesis may influence the electrical properties of the resulting materials, great care has been taken to exclude them from the final products.

Experimental

Materials

PANI in its emeraldine base form was obtained from Neste Oy Chemicals. C₆₀ (content 99%) was received from the Kurchatov Institute Physical Chemistry Synthesis Group. Cadmium hydroxide hydrate [Cd(OH)₂·xH₂O], trifluoromethanesulfonic acid, copper(II) trifluoromethanesulfonate [Cu(CF₃SO₃)₂], and lithium sulfide were purchased from Aldrich Chemical Co. or Fluka, and *N*-methylpyrrolidone (NMP) was obtained from

Sigma. Cadmium laurate is commercially available from SATTVA Chemical Co. (Stamford, CT). All chemicals were used as received, except PANI, which was dried under a dynamic vacuum of 10^{-3} mbar for 24 h prior to use.

Analyses

Metal contents were determined by atomic absorption spectroscopy by the analytical service of the Laboratory of Inorganic Chemistry of ETH Zürich (for the Cd and Cu analysis of nanocomposites, powders of the latter were dissolved in 0.1 M HNO₃ to yield *ca.* 5 ppm Cd or Cu in the solution). X-Ray diffraction patterns of powders were taken with Cu-K α radiation ($\lambda = 1.542 \text{ \AA}$) using a Siemens D5400 diffractometer. KBr pellets were used for FTIR absorption spectra, which were recorded on a Bruker IFS 66v spectrometer. For electron microscopy (EM) studies, composite samples were redispersed in NMP solution, drops of which were placed onto carbon-coated copper grids and dried at *ca.* 10^{-3} mbar for 3 days; EM images were obtained with a Philips EM 301 electron microscope. UV/VIS absorption spectra were recorded on a Perkin Elmer Lambda 900 instrument.

Synthesis of cadmium trifluoromethanesulfonate

Cadmium hydroxide hydrate (29.0 g, 0.16–0.17 mol) was suspended in distilled water (200 mL). Trifluoromethanesulfonic acid (50.0 g, 0.33 mol) was slowly added and the mixture heated to 70 °C for 1 h. The pH of the solution was around 5.5 to 6.0, indicating that sufficient trifluoromethanesulfonic acid had been added to neutralize the hydroxide ions released from the cadmium hydroxide hydrate. After cooling to room temperature (RT), the solvent was evaporated. The crude product was dried under vacuum (*ca.* 10^{-3} mbar) for 12 h, dissolved in ethanol (750 mL), and the solution filtered through Celite. The solvent was evaporated, and the residue was dissolved in a mixture of toluene (750 mL) and ethanol (85 mL) at 70 °C. Thereafter, the resulting solution was cooled to *ca.* 4 °C. After 24 h, white crystals appeared, which were collected by filtration and dried under vacuum (*ca.* 10^{-3} mbar) for 24 h, yielding 37.0 g (0.090 mol, *ca.* 55%) of Cd(CF₃SO₃)₂. Analysis: C found 5.87, expected 5.85%; H and N below detection limit.

Synthesis of PANI–CdS nanocomposites

Nanocomposites of CdS and PANI were prepared from solutions with different CdS/PANI weight ratios (r_{Cd} , calculated on the basis of quantitative conversion of cadmium trifluoromethanesulfonate to CdS) ranging from 0.2 to 5. As an example, the detailed preparation procedure for a material prepared from a solution with $r_{\text{Cd}} = 2.0$ is given; all other composites were synthesized in analogy by variation of the Cd(CF₃SO₃)₂ and, concomitantly, Li₂S content (Table 1). Thus, for the material with $r_{\text{Cd}} = 2.0$, PANI (1.50 g) was dissolved in NMP (50 mL) and the solution was stirred for 24 h, filtered, and used as a stock solution. An aliquot of the latter (4.2 mL, containing 126 mg PANI) and a solution of cadmium trifluoromethanesulfonate (716.1 mg, 1.74 mmol) in NMP (5 mL) were mixed. To the resulting solution, a solution of lithium sulfide (80.2 mg, 1.75 mmol) in NMP (10 mL) was rapidly added under vigorous stirring; and the color of the initially deep blue solution immediately turned green. The subsequent addition of ethanol (200 mL) caused a solid to precipitate, which was filtered off. A fraction of this precipitate was dried at *ca.* 10^{-3} mbar for 24 h and analyzed (Table 1; fluorine and lithium contents were below the detection limit of 0.1%). For the preparation of films, the remaining undried precipitate was dissolved in NMP to yield a solution which contained about 2% w/w PANI. Films of about 2 μm (for UV/VIS absorption measurements) and about 100 μm in thickness (for photovoltaic measurements) were prepared by

Table 1 Analytical data for selected CdS–PANI and Cu₂S–PANI nanocomposites obtained by co-precipitation from NMP solutions containing different CdS/PANI (r_{Cd}) and Cu₂S/PANI (r_{Cu}) ratios, respectively. C, H, and N contents were obtained from organic elemental analysis and metal contents by atomic absorption spectroscopy. Metal sulfide contents were calculated from the metal contents (for details, see text). Note that some NMP remained in the composites, and that the carbon and nitrogen contents reflect the lower limit of these elements, since the combustion of PANI appears to be incomplete under the conditions applied here. Hence, the metal contents were used for the calculation of the weight and volume fractions of metal sulfides

CdS–PANI			
	$r_{\text{Cd}}=0.18$	$r_{\text{Cd}}=2.0$	$r_{\text{Cd}}=3.1$
C (% w/w)	61.79	27.28	21.18
H (% w/w)	5.54	2.98	2.76
N (% w/w)	12.66	5.40	4.59
Cd (% w/w)	12.4	46.5	49.8
CdS (% w/w)	16.0	59.7	64.0
CdS (% v/v)	3.8	24	27
Cu ₂ S–PANI			
	$r_{\text{Cu}}=0.23$	$r_{\text{Cu}}=1.4$	$r_{\text{Cu}}=2.3$
C (% w/w)	56.00	32.16	29.11
H (% w/w)	5.55	3.66	3.80
N (% w/w)	11.55	6.36	5.09
Cu (% w/w)	13.6	33.6	42.2
Cu ₂ S (% w/w)	17.0	42.0	52.8
Cu ₂ S (% v/v)	3.5	11	17

casting the metal sulfide–PANI mixtures, which were filtered through a Teflon[®] filter (0.2 μm pore diameter), on the desired substrate (*vide infra*) and subsequently dried under a vacuum of 4 mbar at 40 °C for 1–3 days. Film thicknesses were measured with a Tencor Alpha Step 200 profilometer.

Preparation of tetrakis(acetonitrile)copper(I) trifluoromethanesulfonate

[Cu(CH₃CN)₄]CF₃SO₃ was prepared from commercially available Cu(CF₃SO₃)₂ (Fluka) according to a previously published procedure.³¹ The white [Cu(CH₃CN)₄]CF₃SO₃ crystals obtained were stored under acetonitrile prior to use, since they are known to slowly oxidize in the dry state when exposed to air.³¹

Preparation of PANI–Cu₂S nanocomposites

Cu₂S–PANI nanocomposites were obtained in analogy to the CdS–PANI nanocomposites described above, but using [Cu(CH₃CN)₄]CF₃SO₃ instead of Cd(CF₃SO₃)₂. Analytical data of the chemical compositions of the copper-based nanocomposites are given in Table 1; fluorine and lithium contents were below the detection limits of 0.1%.

Photovoltaic experiments

For photovoltaic experiments, nanocomposite or neat PANI films with thicknesses of *ca.* 100 μm were prepared according to the above procedures on glass substrates, onto which an aluminium electrode had been thermally evaporated. On top of the PANI–CdS films, a Cd_{1–x}Zn_xO electrode was deposited by magnetron sputtering of a cadmium target (to which 10% w/w zinc was added as a dopant) in the presence of N₂ and O₂. In some cases, an additional intermediate layer (*ca.* 50 nm) of C₆₀ was introduced by thermal evaporation at a temperature of *ca.* 400 °C between the semiconducting polymer and the Cd_{1–x}Zn_xO electrode. *I–V* curves of such devices were measured in the dark and under the illumination of a tungsten–halogen lamp with an incident power of 100 mW cm^{–2}.

Results and discussion

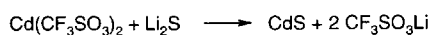
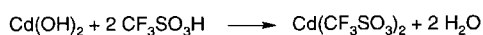
Preparation of CdS–PANI systems

The preparation of nanocomposites based on PANI in its emeraldine base (EB) state was accomplished in *N*-methylpyrrolidone, one of the few conventional, non-acidic solvents for PANI. Although commercially available cadmium salts such as cadmium 2,4-pentanedionate (cadmium acetylacetonate) and cadmium laurate exhibit insufficient solubility in NMP under the conditions applied here, cadmium trifluoromethanesulfonate was found to be a suitable, NMP-soluble starting compound for the *in situ* preparation of CdS. Cadmium trifluoromethanesulfonate was prepared from cadmium hydroxide hydrate and was further converted to CdS with Li₂S in NMP solution in the presence of PANI (Scheme 1). H₂S could also be used instead of Li₂S, however, handling H₂S is not particularly appealing and, in addition, CF₃SO₃H would arise as an undesirable byproduct.

Solutions containing *in situ*-prepared CdS and PANI in NMP with CdS/PANI weight ratios (r_{Cd}) between 0.05 and 4.7 show two distinctive absorption bands in their UV/VIS spectra with maxima at 340 and 637 nm, which coincide with those of neat PANI.^{32–34} With increasing CdS/PANI ratio, however, the peak centered around 340 nm becomes substantially broadened, since the absorption of colloidal CdS^{18,35} overlaps with that of PANI. At 637 nm, the absorption of CdS nanoparticles is negligible, even at the highest CdS/PANI ratios investigated here³⁶ and, consequently, the peak at 637 nm was not affected significantly by the presence of CdS in freshly prepared solutions. We should, however, note that a hypsochromic shift was observed for CdS–PANI solutions which were stored for several days in ambient light or in the dark. For example, the absorption maximum of a sample with r_{Cd} = 2.0 shifted by *ca.* 30 nm during 7 days exposure to ambient light. The shifts were similar for samples kept in ambient light or in the dark and were more pronounced for higher CdS/PANI ratios, indicating a slow degradation process *in solution*.

Nanocomposites were isolated from the above discussed CdS–PANI solutions by co-precipitation with ethanol. Gratifyingly, the side product of the reaction, CF₃SO₃Li, is soluble in the resulting solvent mixture and, thus, its concentration in the nanocomposites was below the detection limit (see Experimental section). After filtering off the nanocomposites, the filtrate was colorless or only slightly blue (in particular for low CdS/PANI ratios), indicating that PANI precipitated essentially quantitatively. The colloidal CdS did not precipitate completely under the conditions applied here; 6 and 7%, respectively, remained in solution when nanocomposites with 3.8 and 27% v/v CdS (see Table 1, r_{Cd} = 0.18 and 3.1) were prepared, as determined by atomic absorption spectroscopy (AAS). Based on the Cd content determined by AAS and the densities of CdS (4.82 g cm⁻³³⁷) and the organic matrix (approximated to 1 g cm⁻³), we estimate the volume contents of CdS in the above samples to about 4 and 27%, respectively. It should be noted in this context that PANI samples prepared from NMP solutions always contain a considerable amount of NMP, which cannot be removed simply by heating or drying in vacuum.³⁸ As a consequence, all nanocomposites prepared here contain some remaining solvent, as evident from infrared (IR) spectra. A signal appeared at 1664 cm⁻¹, in the C=O stretching region, which was absent in PANI before NMP exposure but corresponds rather well to the peak at 1682 cm⁻¹ in neat NMP.

X-Ray diffraction (XRD) patterns of CdS–PANI powders



Scheme 1 Synthesis of CdS.

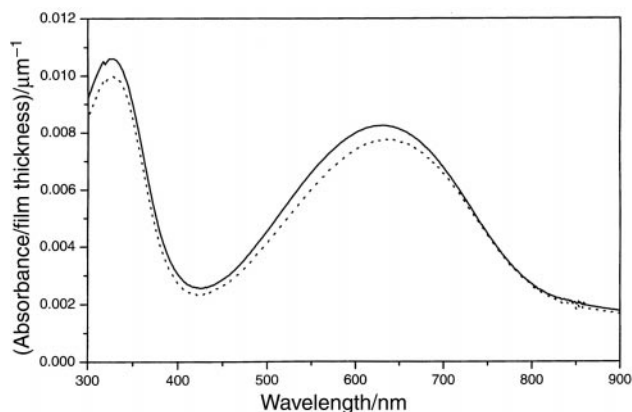


Fig. 1 UV/VIS absorption spectra of a neat PANI film (solid line) and a PANI–CdS nanocomposite film (dotted line) containing 27% v/v CdS.

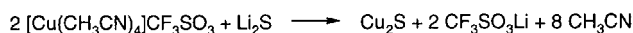
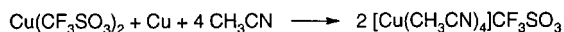
show broad peaks at 2θ values of 27° and *ca.* 47° with a shoulder around 53°, which are in good agreement with the previously reported patterns of other nanocomposites containing CdS.²⁰ These signals have been attributed to the (111), (220) and (311) planes of CdS.²⁰ An additional signal at 2θ = 25° in the pattern of the PANI–CdS nanocomposites, which overlaps with the peak at 27°, is assigned to the PANI matrix, since a signal at this position is also visible in XRD patterns of neat PANI. The CdS particle diameters, as estimated with the Scherrer equation from the line width in the XRD patterns,³⁹ are in the range 1–2 nm for all nanocomposites prepared in this work. This dimension is consistent with the fact that the particles could hardly be detected by transmission electron microscopy (TEM).

In order to prepare nanocomposite films, freshly precipitated, undried CdS–PANI nanocomposite powder was redissolved in NMP and films with thicknesses of 2 and 100 µm were produced by solution casting. The maxima in the UV/VIS absorption spectra of these films did not significantly differ from those of the freshly prepared solutions and of pure PANI films (Fig. 1); gratifyingly, the above-mentioned change in the optical absorption characteristics with time, observed in solution upon storage, were not distinctly observed in the solid state; PANI–CdS nanocomposites were found to be stable in air for a period of a few days at least. Since the optical absorption of PANI in the composite films was not appreciably affected by the presence of CdS colloids, we conclude that ground state charge-transfer interactions between the polymer and the nanoparticles are negligible.

Preparation of Cu₂S–PANI systems

Nanocomposites of Cu₂S and PANI were prepared analogously to the CdS–PANI nanocomposites described above. The Cu₂S colloids were synthesized *in situ* using [Cu(CH₃CN)₄]CF₃SO₃ as an NMP-soluble copper(I) salt, which was produced according to the reaction shown in Scheme 2. Cu₂S colloids were produced by addition of Li₂S to [Cu(CH₃CN)₄]CF₃SO₃ in an NMP solution of PANI. Interestingly, we observed that PANI stabilized the Cu₂S colloids in the NMP solution; Cu₂S was found to slowly precipitate in the absence of PANI.

UV/VIS absorption spectra of Cu₂S–PANI solutions in NMP showed that the absorption maximum in the visible wavelength range of the emeraldine base was shifted to shorter



Scheme 2 Synthesis of Cu₂S.

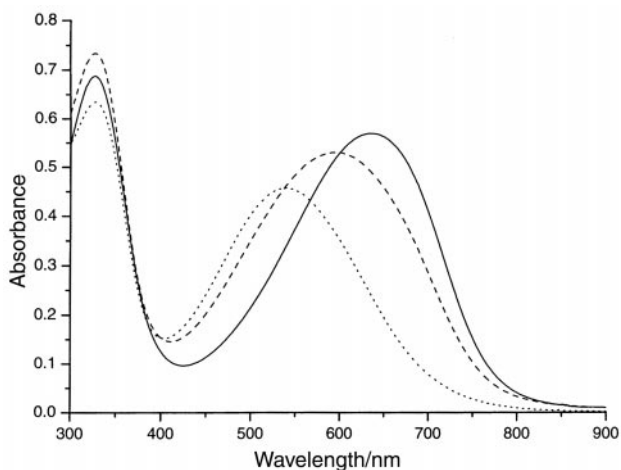


Fig. 2 UV/VIS absorption spectra in NMP of PANI (solid line), a freshly prepared solution of Cu_2S and PANI ($r_{\text{Cu}}=0.23$) (dashed line), and the same solution after storing for 24 h (dotted line).

wavelengths (see Fig. 2). In a freshly prepared solution, the absorption maximum in the presence of Cu_2S appeared at 592 nm (at a $\text{Cu}_2\text{S}/\text{PANI}$ weight ratio, r_{Cu} , of 0.23) compared to 637 nm for the pristine PANI solution. As a consequence, the color of the originally blue PANI solutions changed to purple. The shift in the absorption maximum became more pronounced after 24 h (Fig. 2), when the absorption maximum decreased to 542 nm, indicating that the Cu_2S -PANI solutions investigated here also exhibit limited stability.

As in the case of the CdS-PANI nanocomposites, Cu_2S -PANI nanocomposites were obtained by co-precipitation upon addition of ethanol to the NMP solutions. Nanocomposites with Cu_2S contents of 17.0, 42.0 and 52.8% w/w were produced (Table 1), corresponding to 3.5, 11, and 17% v/v, respectively, assuming a density for Cu_2S of 5.6 g cm^{-3} .³⁷ A slightly purple or blue color in the filtered solution indicated that the components did not precipitate quantitatively. After precipitation and filtration of a nanocomposite containing, e.g., 17.0% w/w Cu_2S , around 2% of the originally used Cu_2S remained in the filtrate, as measured by AAS. For these materials as well, IR spectra indicated the presence of NMP. The characteristic XRD peaks of Cu_2S , reported at 2θ values of 22, 25 and 38° ,⁴⁰ were also found in the Cu -PANI samples; however, these peaks appeared extremely broad, suggesting Cu_2S diameters of below 2 nm, in agreement with TEM images, where the particles are not unambiguously resolved. A much sharper signal at $2\theta=25^\circ$ is attributed to PANI (*vide supra*).

Similar to the behavior in solution, the absorption characteristics in the solid nanocomposite films dramatically altered with time in the presence of Cu_2S , which caused an irreversible decomposition of the material. The absorption maximum of the band initially centered around 637 nm shifted to 540 nm in ambient atmosphere within 10 h, as shown in Fig. 3 for the example of a nanocomposite with 17.0% w/w Cu_2S ; materials with higher Cu_2S contents exhibited essentially similar behavior. Thus, while Cu_2S -PANI nanocomposites can indeed be successfully prepared with the methodology introduced here, these materials seem to be of limited use for practical applications due to their restricted stability.

Photovoltaic characteristics

Preliminary investigations on the photovoltaic characteristics of the new CdS-PANI nanocomposites were conducted on devices consisting of an Al cathode that was deposited on glass by evaporation, a solution-cast nanocomposite layer of ca. 100 μm thickness and a semi-transparent $\text{Cd}_{1-x}\text{Zn}_x\text{O}$ anode. In addition, we investigated devices that also contained a thin

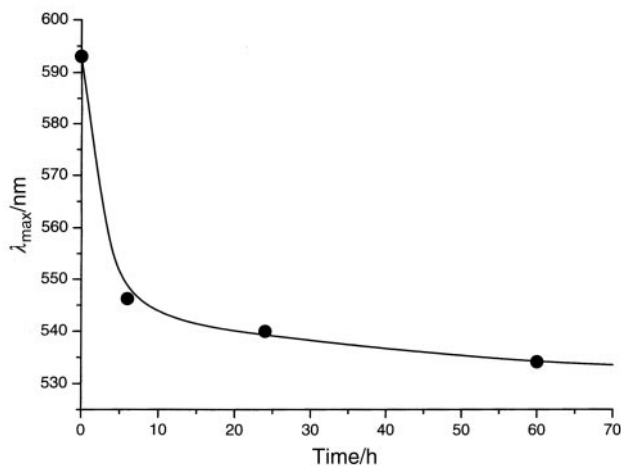


Fig. 3 Maximum of the UV/VIS absorption band (λ_{max}) of a Cu_2S -PANI nanocomposite film ($r_{\text{Cu}}=0.23$) as a function of time. The line is an arbitrary guide for the eye.

layer of C_{60} between the nanocomposite and the $\text{Cd}_{1-x}\text{Zn}_x\text{O}$ contact.

The I - V curves of devices containing the 27% v/v CdS/PANI composite measured under illumination and in the dark are shown in Fig. 4. For comparison, we have also included in Fig. 4 the data of a reference device with neat PANI. While in case of the latter structure the I - V curves reflect only a small rectification, introduction of CdS nanoparticles led to devices which exhibit a pronounced rectifying behavior in the absence of C_{60} , as is evident from Fig. 4. The dependencies of the open

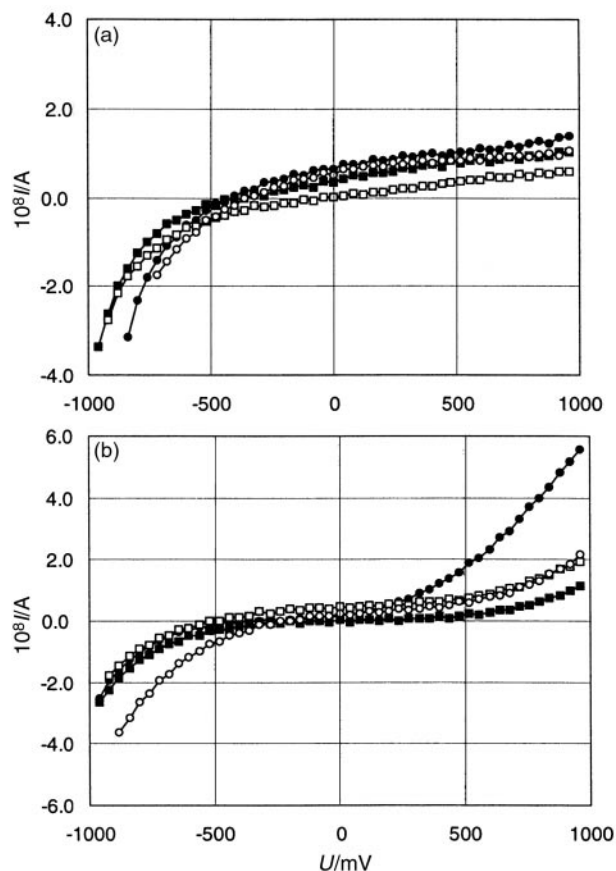


Fig. 4 Current-voltage (I - V) curves of Al/nanocomposite/ $\text{Cd}_{1-x}\text{Zn}_x\text{O}$ (filled symbols) and Al/nanocomposite/ $\text{C}_{60}/\text{Cd}_{1-x}\text{Zn}_x\text{O}$ (open symbols) photovoltaic cells based on (a) neat and (b) 27% v/v CdS-containing polyaniline films. Data were recorded in the dark (squares) and under illumination (circles) of the devices using a tungsten-halogen lamp with an incident radiation power of 100 mW cm^{-2} .

Table 2 Dependencies of open circuit photovoltage (U_{oc}) and short circuit photocurrent (I_{sc}) of Al/nanocomposite/Cd_{1-x}Zn_xO (filled symbols) and Al/nanocomposite/C₆₀/Cd_{1-x}Zn_xO (open symbols) photovoltaic devices on the CdS nanoparticle concentration. Data were recorded under illumination of the devices using a tungsten-halogen lamp with an incident radiation power of 100 mW cm⁻²

CdS content (% v/v)	Without C ₆₀		With C ₆₀	
	U_{oc}/mV	$I_{sc}/nA\ cm^{-2}$	U_{oc}/mV	$I_{sc}/nA\ cm^{-2}$
0	-54	-27	202	40
3.8	-44	-22	74	322
24	-112	-85	90	89
27	-297	-118	117	11

circuit voltage, U_{oc} , and the short circuit current, I_{sc} , of the Al/nanocomposite/Cd_{1-x}Zn_xO and Al/nanocomposite/C₆₀/Cd_{1-x}Zn_xO structures on the CdS concentration are presented in Table 2. In the case of the Al/nanocomposite/Cd_{1-x}Zn_xO devices, high CdS concentrations caused a significant increase in both U_{oc} and I_{sc} with increasing CdS content. For the nanocomposite with 27% v/v CdS, appreciable U_{oc} and I_{sc} values of -295 mV and -1.18×10^{-7} A cm⁻², respectively, were found. This behavior reflects efficient charge separation of the photogenerated charge carriers at the CdS-PANI interface. The photogenerated holes become mobile and can be transported to the anode through the polymer layer. The Al-nanocomposite interface represents a Schottky barrier, which apparently is lowered with increasing CdS concentration, leading to the observed increase in photocurrent.

A significant charge separation and, concomitantly, appreciable values for U_{oc} and I_{sc} were also observed at low CdS concentrations in Al/nanocomposite/C₆₀/Cd_{1-x}Zn_xO structures, but with the opposite sign for U_{oc} (Table 2). In this case, increasing the CdS concentration to 27% v/v caused a substantial reduction of the short circuit current. The C₆₀ layer is characterized by a high electron affinity⁶ and, obviously, introduces an additional Schottky barrier which renders the dependency of U_{oc} and I_{sc} on the CdS content more complex. The two Schottky barriers in this system rectify in opposite directions and, as a consequence, partially compensate each other. As the data reflect, the extent of the compensation and the resulting net photocurrent effect strongly depend on the CdS concentration.

Conclusions

In summary, we have shown that nanocomposites of polyaniline and inorganic semiconductors can readily be prepared from PANI solutions in NMP which contain metal trifluoromethanesulfonates as NMP-soluble precursors. The latter easily react with Li₂S to form colloidal metal sulfides. As first examples, materials were prepared with CdS or Cu₂S particles of diameters in the range 1–2 nm. The nanocomposites with CdS seem to be reasonably stable under ambient conditions and exhibit photovoltaic effects. In contrast, nanocomposites containing Cu₂S degraded and are, therefore, of limited practical use.

Acknowledgements

D. G., A. V. and D. Z. acknowledge financial support from ICMR Co., Japan.

References

- 1 E. T. Kang, K. G. Neoh and K. L. Tan, *Prog. Polym. Sci.*, 1998, **23**, 277.
- 2 P. F. Hutten and G. Hadziioannou, in *Handbook of Organic*

- 3 *Conductive Molecules and Polymers*, ed. H. S. Nalwa, John Wiley & Sons, Chichester, 1997, vol. 3, p. 2.
- 4 B. O'Regan and M. Grätzel, *Nature*, 1991, **353**, 737.
- 5 Y. Wang and N. Herron, *Chem. Phys. Lett.*, 1992, **200**, 71.
- 6 B. O. Dabbousi, M. G. Bawendi, O. Onitsuka and M. F. Rubner, *Appl. Phys. Lett.*, 1995, **66**, 1316.
- 7 N. C. Greenham, X. Peng and A. P. Alivisatos, *Phys. Rev. B*, 1996, **54**, 17628.
- 8 W. U. Huynh, X. G. Peng and A. P. Alivisatos, *Adv. Mater.*, 1999, **11**, 923.
- 9 D. Tsamouras, E. Dalas, S. Sakkopoulos and E. Vitoratos, *Appl. Surf. Sci.*, 1993, **65**, 388.
- 10 Y. Wang and N. Herron, *J. Lumin.*, 1996, **70**, 48.
- 11 Y. Wang, *Stud. Surf. Sci. Catal.*, 1996, **103**, 277.
- 12 N. P. Gaponik and D. V. Sviridov, *Ber. Bunsen-Ges. Phys. Chem.*, 1997, **101**, 1657.
- 13 W. Feng, E. Sun, A. Fujii, H. Wu, K. Niihara and K. Yoshino, *Bull. Chem. Soc. Jpn.*, 2000, **73**, 2627.
- 14 S. Pethkar, R. C. Patil, J. A. Kher and K. Vijayamohan, *Thin Solid Films*, 1999, **345**, 105.
- 15 N. P. Gaponik, D. V. Talapin and A. L. Rogach, *Phys. Chem. Chem. Phys.*, 1999, **1**, 1787.
- 16 N. J. Terrill, T. Crowley, M. Gill and S. P. Armes, *Langmuir*, 1993, **9**, 2093.
- 17 S. P. Armes, S. Gottesfeld, J. G. Beery, F. Garzon and S. F. Agnew, *Polymer*, 1991, **32**, 2325.
- 18 M. Wan and J. Li, *J. Polym. Sci., Part A*, 1998, **36**, 2799.
- 19 H. Inoue, R. S. Urquhart, T. Nagamura, F. Griesser, H. Sakaguchi and D. N. Furlong, *Colloids Surf., A*, 1997, **126**, 197.
- 20 V. S. Gurin and M. V. Artemyev, *J. Cryst. Growth*, 1994, **138**, 993.
- 21 J. Wang, D. Montville and K. E. Gonsalves, *J. Appl. Polym. Sci.*, 1999, **72**, 1851.
- 22 A. V. Volkov, M. A. Moskvina, I. V. Karachevtsev, O. V. Lebedeva, A. L. Volynskii and N. F. Bakeev, *Vysokomol. Soedin., Ser. A Ser. B*, 1998, **40**, 970; A. V. Volkov, M. A. Moskvina, I. V. Karachevtsev, O. V. Lebedeva, A. L. Volynskii and N. F. Bakeev, *Chem. Abstr.*, 1999, **131**, 130842k.
- 23 M. Weibel, W. Caseri, U. W. Suter, H. Kiess and E. Wehrli, *Polym. Adv. Technol.*, 1991, **2**, 75.
- 24 L. Zimmermann, M. Weibel, W. Caseri and U. W. Suter, *J. Mater. Res.*, 1993, **8**, 1742.
- 25 T. Kyprianidou-Leodidou, W. Caseri and U. W. Suter, *J. Phys. Chem.*, 1994, **98**, 8992.
- 26 T. Kyprianidou-Leodidou, H.-J. Althaus, Y. Wyser, D. Vetter, M. Büchler, W. Caseri and U. W. Suter, *J. Mater. Res.*, 1997, **12**, 2198.
- 27 B. Z. Tang, Y. Geng, J. W. Y. Lam, B. Li, X. Jing, X. Wang, F. Wang, A. B. Pakhomov and X. X. Zhang, *Chem. Mater.*, 1999, **11**, 1581.
- 28 T. Hirai, M. Miyamoto, T. Watanabe, S. Shiojiri and I. Komasa, *J. Chem. Eng. Jpn.*, 1998, **31**, 1003.
- 29 S. Shiojiri, M. Miyamoto, T. Hirai and I. Komasa, *J. Chem. Eng. Jpn.*, 1998, **31**, 425.
- 30 M. A. Olshavsky and H. R. Allcock, *Chem. Mater.*, 1997, **9**, 1367.
- 31 J. G. Winiarz, L. Zhang, M. Lal, C. S. Friend and P. N. Prasad, *J. Am. Chem. Soc.*, 1999, **121**, 5287.
- 32 W. Caseri, T. Sauer and G. Wegner, *Makromol. Chem., Rapid Commun.*, 1988, **9**, 651.
- 33 L. H. C. Mattoso and A. G. MacDiarmid, in *Polymeric Materials Encyclopedia*, ed. J. C. Salamone, CRC Press, Boca Raton, FL, 1996, vol. 7, p. 5505.
- 34 S. D. Phillips, G. Yu, Y. Cao and A. J. Heeger, *Phys. Rev. B*, 1989, **39**, 10702.
- 35 R. P. McCall, J. M. Ginder, L. M. Leng, H. J. Ye, S. K. Manohar, G. E. Asturias, A. G. MacDiarmid and A. J. Epstein, *Phys. Rev. B*, 1990, **41**, 5202.
- 36 T. Hirai, M. Miyamoto and I. Komasa, *J. Mater. Chem.*, 1999, **9**, 1217.
- 37 H. S. Zhou, I. Honma, H. Komiyama and J. W. Haus, *J. Phys. Chem.*, 1993, **97**, 895.
- 38 *Handbook of Chemistry and Physics*, ed. D. R. Lide, CRC Press, Boca Raton, FL, 1995.
- 39 M. Angelopoulos, G. E. Asturias, S. P. Ermer, A. Ray, E. M. Scherr and A. G. MacDiarmid, *Mol. Cryst. Liq. Cryst.*, 1988, **160**, 151.
- 40 P. Scherrer, *Nachr. K. Ges. Wiss. Göttingen, Math.-Phys. Kl.*, 1918, 98.
- 41 N. L. Fainer, Yu. M. Rumyantsev, M. L. Kosinova, G. S. Yur'ev, E. A. Maksimovskii, S. M. Zemskova, S. V. Sysoev and F. A. Kuznetsov, *Inorg. Mater.*, 1998, **34**, 1049.